

## Molecular dynamics simulation of the adsorption properties of graphene oxide/graphene composite for alkali metal ions

Jianping Zeng<sup>a,b</sup>, Yan Zhang<sup>a</sup>, Yuhang Chen<sup>a</sup>, Zijie Han<sup>a</sup>, Xinmiao Chen<sup>a</sup>, Yue Peng<sup>a</sup>, Long Chen<sup>a</sup>, Song Chen<sup>a,\*</sup>

<sup>a</sup> School of Chemistry and Chemical Engineering, Yancheng Institute of Technology, Yancheng, 224051, China

<sup>b</sup> Research School of Chemistry, The Australian National University, Canberra, Australian Capital Territory, 2601, Australia



### ARTICLE INFO

**Keywords:**  
Graphene oxide/graphene composite  
Molecular dynamics  
Adsorption  
Interaction energy  
Diffusion coefficient  
Radial distribution function

### ABSTRACT

As one of the effective methods to remove heavy metals, graphene (G) composite adsorption technology is irreplaceable in water pollution control and water purification, but its adsorption mechanism is not clear. Materials Studio (MS) software was used to simulate the molecular dynamics of the interaction between graphene oxide/graphene (GO/G) composite and alkali metal ion ( $M^+$ ). Based on the calculation of the interaction energy, diffusion coefficient and radial distribution function (RDF), The adsorption law of GO/G on  $M^+$  was investigated and its mechanism was revealed. It provides a theoretical basis for the research and development of the adsorption performance of G composite electrode. The calculated results show that the interaction energy between different  $M^+$  and GO/G is negative, indicating that the interaction between them is mutual attraction. The energy of GO/G composites and the total energy of  $M^+$ -GO/G increase with the increase of  $M^+$  radius. The larger the hydrated ion radius of  $M^+$  is, the larger the diffusion coefficient is.  $Cs^+$  diffusion coefficient is slightly lower than rubidium. According to RDF analysis,  $M^+$ -GO and  $M^+ - O$  (GO) both have bonding within 3.5 Å and non-bonding after 3.5 Å, and the non-bonding interaction of  $M^+$ -GO is greater. However, the bonding interaction between  $M^+$ -O(GO) is larger than the non-bonding interaction, indicating that there are bonding and non-bonding interactions in the system when GO/G composite adsorb  $M^+$ . The interaction between  $M^+$  and GO surface is mainly provided by non-bonding interaction, while the interaction between  $M^+$  and O atoms of GO surface is mainly provided by bonding interaction.

### 1. Introduction

In the electric adsorption technology, desorption effect can be achieved after the electrode material is adsorbed to saturation state by reverse voltage connection or short circuit connection of electrodes and the electrode materials is cleaned with water [1]. The whole process of electric desorption does not use auxiliary reagents, and no by-products are generated. It is a green separation technology with great development prospects [2]. The core part of the electric adsorption device is the porous electrode, so the performance of the porous electrode greatly restricts the performance of the electric adsorption device. Improving the specific surface area and conductivity of the electrode is the key to improve the adsorption capacity of the electrode. At present, most of the electroadsorption electrodes are carbon materials with large specific surface area, such as graphene (G) and its derivatives, carbon aerogel, carbon nanotubes and carbon fiber [3]. These carbon materials have

excellent electrical conductivity and relatively large specific surface area, providing a large number of adsorption sites for ion adsorption. Electric adsorption technology has unique advantages in desalting saline wastewater, and alkali metal ions ( $M^+$ ) are the most common cations in water, so it is of great significance to investigate the electric adsorption behavior of alkali metal ions [4].

Graphene oxide (GO) is a derivative of G, which has attracted a lot of attention due to its large specific surface area, abundant oxygen-containing functional groups existing at the edge of carbon framework structure, and easy surface modification and modification. So far, researchers have used GO and its composites with strong adsorbability to conduct more experimental studies in the control of water pollution and purification of water quality [5–10]. Because the interaction between the adsorbed substance and GO and its derivatives includes physical, chemical and physicochemical processes. There are some higher-order continuum theories (nonlocal elasticity, strain gradient elasticity,

\* Corresponding author.

E-mail address: [abcjp768472@163.com](mailto:abcjp768472@163.com) (S. Chen).

couple stress theories) for mechanical behaviour of such a nano/micro scaled modeling [11,12]. However, there are relatively few studies on the mechanism of interaction at the molecular and atomic level.

Molecular Dynamics (MD) simulation is a molecular simulation method based on classical Newtonian equations, which is widely used in drug design, materials and biology. In the field of environment, MD simulation can be used to study the adsorption behavior of target pollutant molecules on various material interfaces [13]. A large number of studies have used MD simulation method to explore the interaction mechanism between target pollutants and adsorbed materials in the adsorption process at the molecular level, and the experimental results under different conditions have been well explained and predicted. Zahra Taheri et al. [14] conducted MD researches on the adsorption and diffusion behavior of methane on GO and obtained adsorption isotherms at different temperatures. Li et al. [15] conducted MD study on rapid evaporation of water on graphene-graphene oxide surface. The results show that water/graphene and water/graphite oxide systems store more energy during evaporation than pure water systems. The hydroxyl group on the graphene oxide surface reduces the attraction between water molecules and the graphene oxide surface. Izadkhah et al. [16] studied the effect of GO nanosurfaces on the stability and thermal conductivity of nanofluids using the MD method, and the results confirmed the stability of water/GO nanofluids, while adding glycol and increasing its content in the base fluid can reduce the stability of nanofluids. Yang et al. [17] [1,18] [1,19] used MD to study the interlaminar thermal property of graphene oxide films. They considered the effect of vacancy defect on the thermal conductance of the interface. The results showed that the interfacial heat transfer efficiency of graphene oxide films strengthens with the increasing ratio of the vacancy defect, and the thermal conductivity of GO increases with the model length. Wang et al. [19] investigated interfacial characteristics between graphene oxide (GO) and calcium silicate hydrate (C-S-H) composite using MD simulations. They studied effects of functional group types (carboxyl and hydroxyl functional groups) and water content on the interfacial bonding strength. The simulation results revealed that the interfacial bonding strength between GO and C-S-H is enhanced significantly than that of between pristine graphene sheet (GN) and C-S-H. Zheng et al. [20] explored the prospect of using layered GO membranes to separate cadmium ions from water by molecular dynamics. The results indicate that the effects of the interlayer spacing and offset value on the salt rejection rate are much greater than the corresponding effects on water permeability. The radial distribution function and coordinate number indicate that Cd<sup>2+</sup> is surrounded by two hydration shells. The second shell is more flexible so that it allows the loss of several water molecules to enable Cd<sup>2+</sup> to pass through the membrane.

The above studies mainly involved MD simulation of interactions related to GO, but did not study the MD process of adsorption of alkali metal ions on GO/G surface. This paper aimed to simulate the adsorption process of M<sup>+</sup> on GO/G composite electrode using MD methods. The adsorption law of GO/G electrode materials on M<sup>+</sup> was discussed at molecular and atomic level, and the adsorption mechanism was revealed. It provides a theoretical basis for the research and development of the adsorption of M<sup>+</sup> on GO/G electrode.

## 2. Modeling and simulation methods

It is difficult to determine the strength and mechanism of interfacial molecular interactions by traditional experimental methods. Meanwhile, with the development of computers and algorithms, molecular simulation shows great potential in dealing with interfacial interactions and revealing microcosmic mechanisms. In contrast to other computational simulation software such as NAMD, GROMACS and LAMMPS, Materials Studio provides a user-friendly simulation environment for in-depth study of the properties and processes of a wide variety of small molecules, nanoclusters, crystals, amorphous and polymer Materials. Using Materials Studio's scientific research and advanced computing

methods, users can easily build 3D molecular models for in-depth analysis of organic and inorganic crystals, amorphous Materials and polymers without resorting to third-party software for data processing. In this work, we used the software Materials Studio to establish the interaction between M<sup>+</sup> solution and GO/G and performed molecular dynamics simulations. First, a two-dimensional (2D) G and GO models were constructed. According to Ref. [18,20], hydroxyls (-OH) and (1,2) epoxies (-O-) are the main oxygen-containing functional groups of GO. The structure of GO was obtained by randomly distributing -OH and -O-groups on the surface of G. Both of 2D supercell of GO and G are 14.76 Å × 14.76 Å in size, as shown in Fig. 1. The former contains 72C atoms, 4-OH and 2-O- groups, and the latter 72C atoms. In order to facilitate the analysis of the interaction mechanism, defects were not considered in the GO model in this work. The condensed-phase optimized molecular potential for atomistic simulation studies (COMPASS) Force Field [21–23], which had been adopted in relation to molecular dynamics simulation of GO/G [24,25], was used in geometry optimization and dynamics calculation.

Second, the layered models of interaction between M<sup>+</sup> solution and GO/G composite were constructed. In order to make the solution electrically neutral, equal amounts of Cl<sup>-</sup> ions were added to each M<sup>+</sup> solution. Taking Li<sup>+</sup> as an example, the molecular molecules was the solution layer, the third layer, with the GO and the G structures as the second and the first layer, respectively. model with 5 Li<sup>+</sup>, 5Cl<sup>-</sup> and 278 water. The layered models of interaction between other ions Na<sup>+</sup>, K<sup>+</sup>, Rb<sup>+</sup> and Cs<sup>+</sup>, and GO/G composite were constructed similarly to that of Li<sup>+</sup> ions. When constructing the layered structure, the ions and molecules in solution appeared on either side of the surface of the GO/G complex due to periodic boundary conditions, we added a vacuum layer of 30 Å to the solution layer, so that the solution layer appears on only one side of the surface layer. The initial configurations of MD simulation were obtained by geometric optimization of these five layered models, as displayed in Fig. 2.

Third, MD simulations of the interactive layer models were performed in the NVT (constant number of particles, volume, and temperature) ensemble [25]. According to the process conditions of adsorption of M<sup>+</sup> by biomass carbon aerogel-GO composite electrode [8], the simulation temperature was set as 298 K. The van der Waals interaction of the model systems were calculated based on the cutoff distance, spline width and buffer width of 15.5, 1 and 0.5 Å, respectively. The Ewald summation method which improves a lot the description of electrostatics for a periodic system with respect to a cutoff-based scheme while retaining the reliability of simulated results was used for the electrostatic interaction [26,27]. The coupling to the heating bath to control temperature was carried out using the Berendsen method [28]. To ensure accuracy of computing results in the shortest possible time, in this work, the time step, total simulation time and output per frame are set as 1 fs, 2000 ps and 5000 steps, respectively. The positions and structures of all the H<sub>2</sub>O molecules, alkali metal ions and Cl<sup>-</sup> ions changed obviously during the simulation. Taking the layered model of interaction between 5Rb<sup>+</sup>/5Cl<sup>-</sup>/278H<sub>2</sub>O - GO/G as an example, the molecular configurations at different simulated moments were shown in Fig. 3.

## 3. Results and discussion

### 3.1. Judgment of system balance

Whether the model system between M<sup>+</sup> solution and GO/G composite electrode has reached equilibrium or not was ascertained by the equilibrium criterions of temperature and energy simultaneously [29], i.e., the fluctuations of temperature and energy should be confined to 5–10%. Taking the adsorption of Li<sup>+</sup> as an example, the temperature fluctuation curve during the whole simulation process was shown in Fig. 4 (a),(b) and the kinetic, potential, non-bond and total energies were shown in Fig. 4 (c).

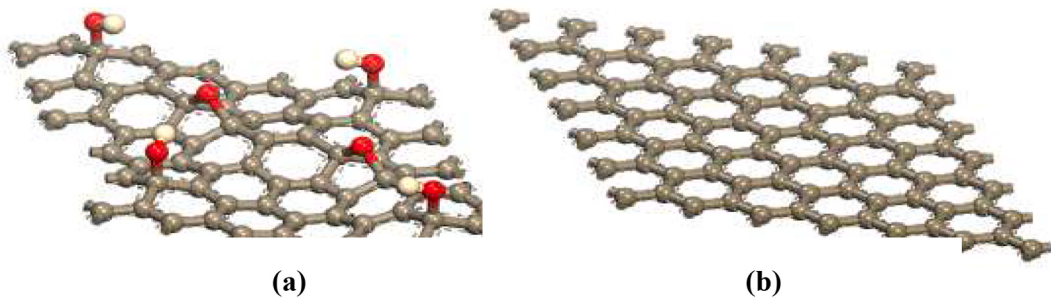


Fig. 1. GO(a) and G(b) structures.

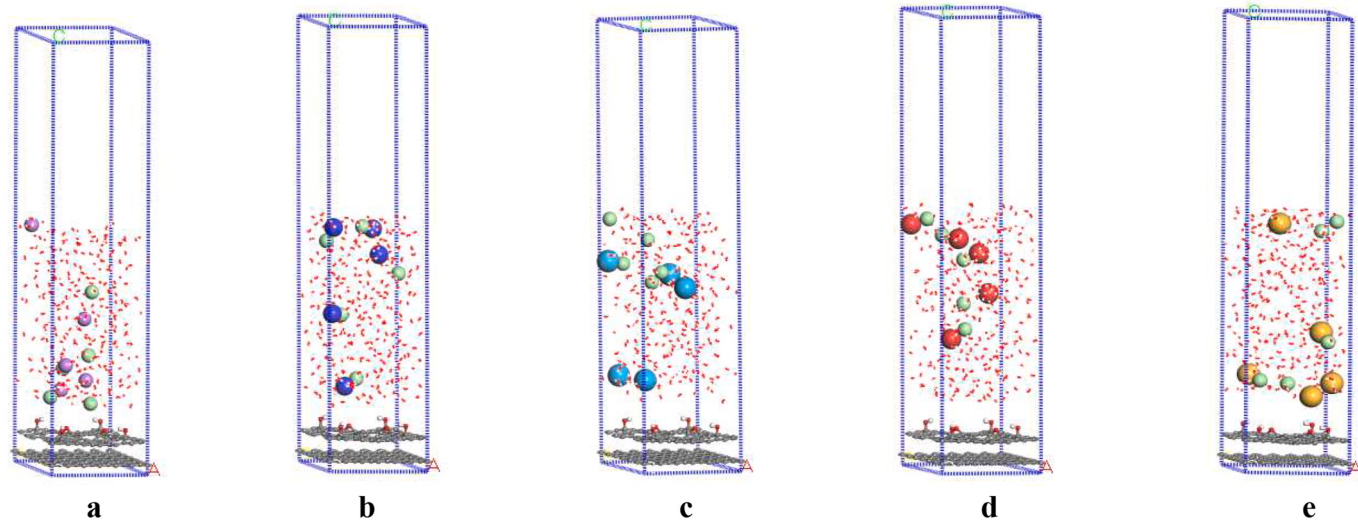
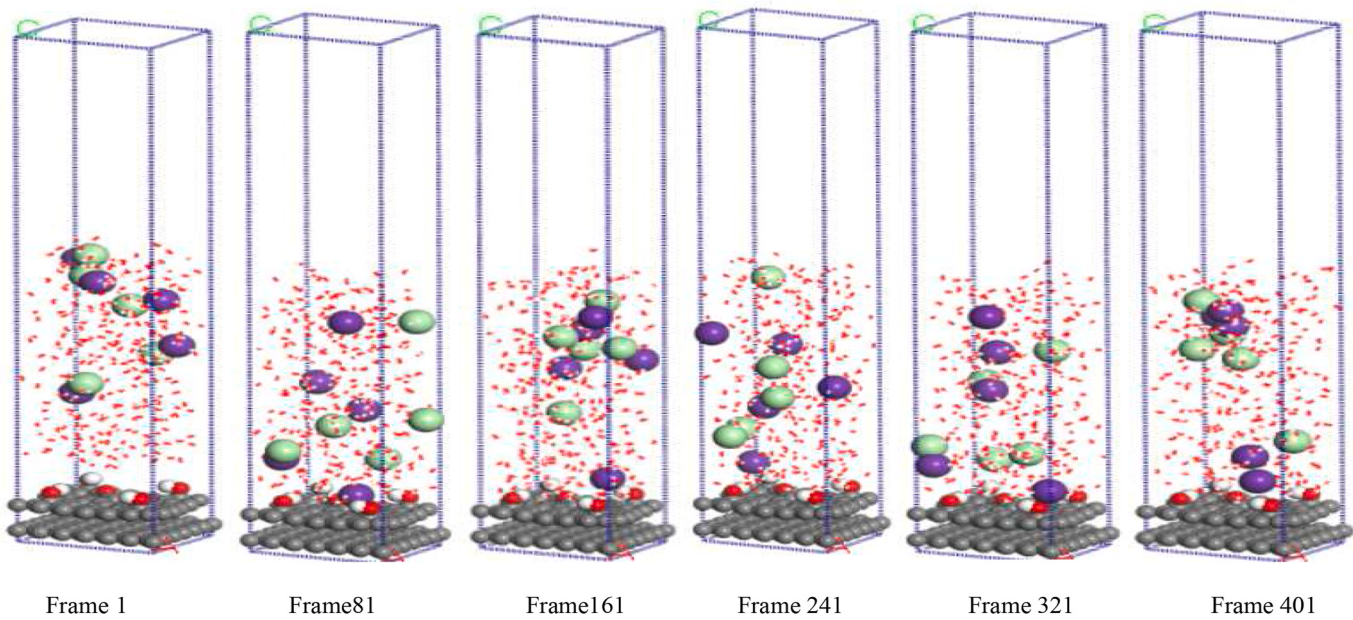
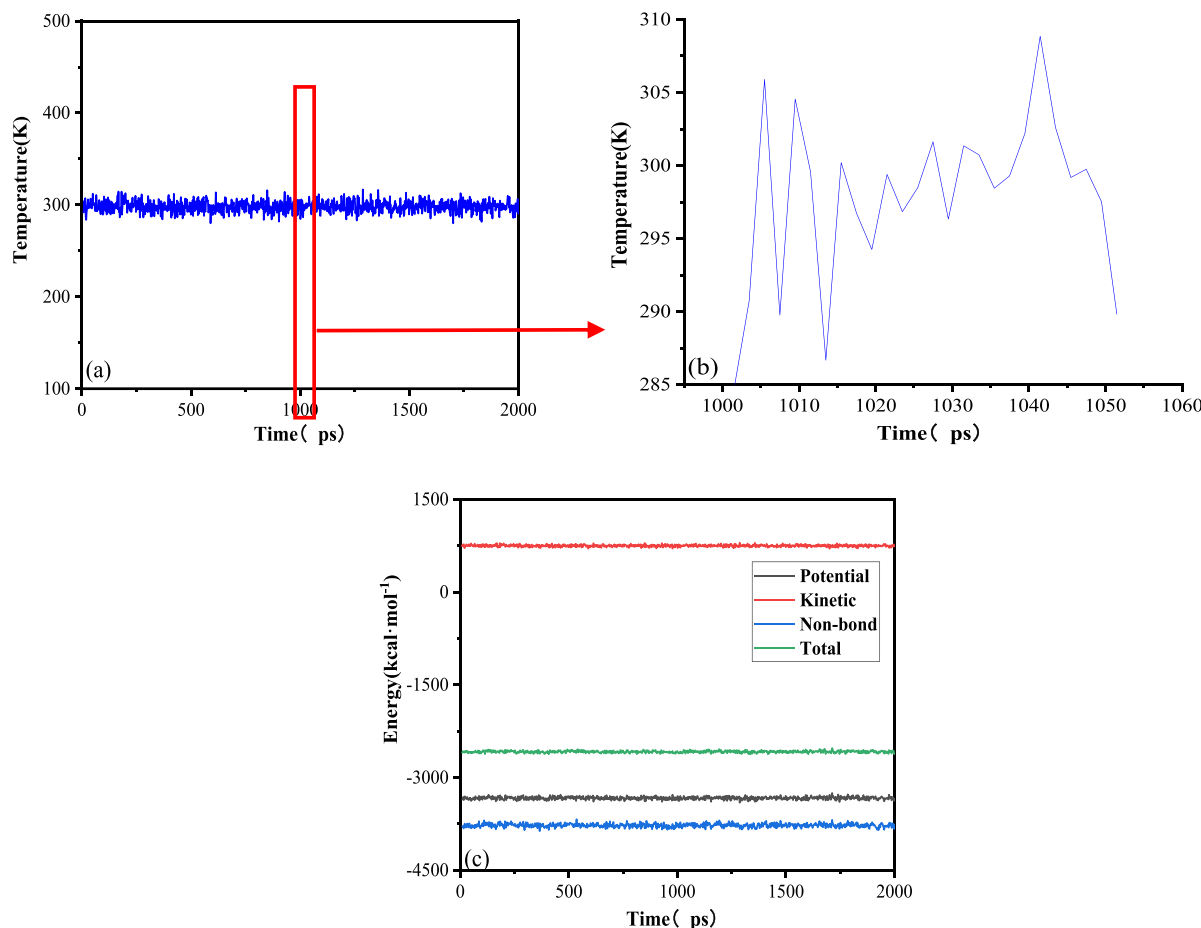


Fig. 2. Initial configurations of the 5 layer models between  $M^+$  solution and GO/G composite. (a,  $5Li^+/5Cl^-/278H_2O$ ; b,  $5Na^+/5Cl^-/278H_2O$ ; c,  $5K^+/5Cl^-/278H_2O$ ; d,  $5Rb^+/5Cl^-/278H_2O$ ; e,  $5Cs^+/5Cl^-/278H_2O$ ). The linear model in Fig. 2 represents  $H_2O$  molecules, the ball and stick models with and without oxygen-containing function groups represents GO and G sheets, respectively; the ball models in purple, blue, cyan, red khaki and green represents  $Li^+$ ,  $Na^+$ ,  $K^+$ ,  $Rb^+$ ,  $Cs^+$ , and  $Cl^-$  ions, respectively. (For interpretation of the references to colour in this figure legend, the reader is referred to the Web version of this article.)

Fig. 3. Molecular configurations of the  $5Rb^+/5Cl^-/278H_2O$  - GO/G model system from MD simulation.



**Fig. 4.** Temperature (a) and energy (c) fluctuation curves in the simulation system of adsorption of lithium ions. (b) is an enlarged view of (a) between 1000 and 1050ps.

As can be seen from Fig. 4a, in the model system of  $\text{Li}^+$  solution, the temperature change is about 298 K, and the temperature fluctuation range is within  $\pm 18.7$  K (Fig. 4b is the temperature fluctuation curve of Fig. 4a between 1000 and 1050ps), which fluctuates around five percent 6.28%. This showed that from the temperature change, the MD model system has reached equilibrium. According to Fig. 4c, the kinetic energy of the model system fluctuates gently at about  $750.3 \text{ kcal mol}^{-1}$  in the process of 2000 ps.

simulation. Potential, non-bond and total energies are all negative, but their fluctuation range is similar to that of kinetic energy, which is also relatively gentle. From the beginning to the end of the simulation, the kinetic, potential, non-bond and total energies in the model system fluctuated up and down within  $750.3$ ,  $-3332.7$ ,  $-3773.4$  and  $2582.3 \text{ kcal mol}^{-1}$ , respectively, within  $\pm 46.5$ ,  $\pm 80.8$ ,  $\pm 96.2$  and  $\pm 56.0 \text{ kcal mol}^{-1}$ . The fluctuation degree is 6.20%, 2.42%, 2.55% and 2.17%, respectively, indicating that the model system is basically in equilibrium state in MD simulation from 0 ps to 2000 ps. Similar to  $\text{Li}^+$ , the fluctuation of temperature and energy curves in the adsorption kinetic process of  $\text{Na}^+$ ,  $\text{K}^+$ ,  $\text{Rb}^+$  and  $\text{Cs}^+$  are within 5–10%, respectively, indicating that the adsorption simulation process of different  $\text{M}^+$  on GO/G composite can reach a balance state.

### 3.2. Interaction energy

The strength of the interaction between  $\text{M}^+ - \text{GO}/\text{G}$  can be characterized by the interaction energy [23]. According to Formula (1), the interaction energy between each substance in the system can be calculated.

$$\Delta E = E_{\text{Total}} - E_{\text{M}^+} - E_{\text{GO}/\text{G}} \quad (1)$$

Where  $E_{\text{Total}}$  is the total energy of the whole alkali metal ions - GO/G,  $E_{\text{M}^+}$  is the energy of all the  $\text{M}^+$  after removing the GO/G composite, all the  $\text{Cl}^-$  and all the  $\text{H}_2\text{O}$  molecules before the MD simulation after the optimization of the layered model system, while  $E_{\text{GO}/\text{G}}$  is the energy of the GO/G composite that removes all the  $\text{M}^+$ , all the  $\text{Cl}^-$  and all the  $\text{H}_2\text{O}$  molecules. The positive value of  $\Delta E$  represents mutual repulsion, the negative value represents mutual attraction, and the magnitude of the value represents the magnitude of the interaction energy. In order to more clearly explore the adsorption of  $\text{M}^+$  solutions on GO/G composite, in this work, we only considered the interaction between  $\text{M}^+ - \text{GO}/\text{G}$  in the model system, and ignored the interactions between  $\text{M}^+ - \text{M}^+$ ,  $\text{M}^+ - \text{Cl}^-$ ,  $\text{Cl}^- - \text{H}_2\text{O}$ ,  $\text{Cl}^- - \text{GO}/\text{G}$ ,  $\text{H}_2\text{O} - \text{H}_2\text{O}$ , and  $\text{H}_2\text{O} - \text{GO}/\text{G}$ .  $E_{\text{Total}}$ ,  $E_{\text{GO}}$  and  $\Delta E$  of different  $\text{M}^+$  interacting with GO/G composite were shown in Table 1.

According to Table 1, all the  $\Delta E$  between different  $\text{M}^+$  and GO/G are negative, ranging from  $17.84$  to  $29.37 \text{ kcal mol}^{-1}$ , indicating that the

**Table 1**  
Interaction energy between  $\text{M}^+ - \text{GO}/\text{G}(\text{kcal}\cdot\text{mol}^{-1})$ .

| Systems       | $E_{\text{Total}}$ | $E_{\text{M}^+}$ | $E_{\text{GO}/\text{G}}$ | $\Delta E$ |
|---------------|--------------------|------------------|--------------------------|------------|
| $\text{Li}^+$ | 20101.56           | 448.70           | 19674.71                 | -21.84     |
| $\text{Na}^+$ | 20337.78           | 372.20           | 19994.95                 | -29.37     |
| $\text{K}^+$  | 20693.47           | 393.37           | 20317.94                 | -17.84     |
| $\text{Rb}^+$ | 21529.57           | 292.16           | 21256.37                 | -18.95     |
| $\text{Cs}^+$ | 22880.34           | 674.99           | 22229.38                 | -24.02     |

adsorption process of  $M^+$  on the GO/G complex surface is mutual attraction. In general, the lower the energy of a system or substance, the more stable it is. It could also be seen from Table 1 that both  $E_{\text{Total}}$  and  $E_{\text{GO}/\text{G}}$  increase with the increase of radius of  $M^+$ . It indicates that the stability of the system of M-GO/G and the GO/G complex surface decreases with the increase of the radius of  $M^+$ , that is, the larger the radius of  $M^+$ , the more unstable the system structure and surface structure. This indicates that the GO/G complex structure has a greater adsorption activity for alkali metal ions with a larger radius. The result is in accordance with the results of Ref. [14] on the adsorption selectivity of the composite GO electrode for  $M^+$ .

### 3.3. Diffusion coefficient

Diffusion is the complete process of the transfer of a substance molecule from a high concentration area to a low concentration area. The interaction between  $M^+$  and GO/G composite electrode involves mass transfer of anions, cations and water molecules in solution. The strength of mass transfer process can be determined by Einstein Formula [30](2). Diffusion coefficient ( $D$ ) [31] is an important physical parameter to describe the mass transfer process and can be used to evaluate the diffusion strength of ions and molecules in solution on composite electrode surface.

$$D = \frac{1}{6N} \lim_{t \rightarrow \infty} \frac{d}{dt} \sum_{i=1}^N \langle [r_i(t) - r_i(0)]^2 \rangle \quad (2)$$

where  $N$  is the number of the particles; and  $r_i(t)$  and  $r_i(0)$  stand for the molecular coordinates of particle  $i$  at  $t$  and initial time, respectively.  $\langle [r_i(t) - r_i(0)]^2 \rangle$  is the mean squared displacement (MSD) of coordinates. In this project, the MSD of the  $M^+$  and solvent water adsorbed on the GO/G composite electrode surface were calculated (Fig. 5 a and b).

Since the diffusion coefficient calculated by Einstein formula means that the diffusion process of material is in a state of linear diffusion, it is necessary to judge the linear part of the  $MSD-t$  curve. It can be seen from Fig. 5a that, in order to compare the diffusion performance of different alkali metal ions in the same time period, We selected the period between 180 ps and 580 ps when linear diffusion is relatively good on this curve, and performed linear fitting of the curves during this period to obtain the fitting equation, and then calculated their respective diffusion coefficients according to Formula (2) (Table 2). According to Fig. 5b, the  $MSD-t$  curves of solvent water molecules in the model system are close to those of different  $M^+$  during the whole simulation time. It shows that there is little difference in diffusion of solvent water molecules in different alkali metal ion systems, because the number of water

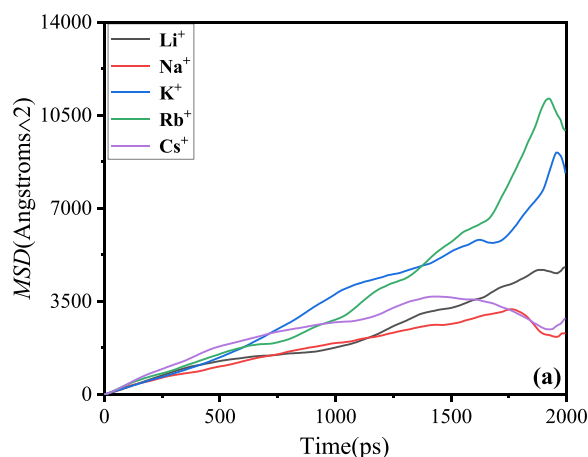


**Table 2**

Fitting equation,  $R^2$ , slope, diffusion coefficient  $MSD-t$  curves of  $M^+$  from 180 to 580ps.

| $M^+$         | Fitting equation       | $R^2$  | slope  | $D$ (Å <sup>2</sup> /ps) |
|---------------|------------------------|--------|--------|--------------------------|
| $\text{Li}^+$ | $y = 2.1129x + 203.15$ | 0.9772 | 2.1129 | 0.352                    |
| $\text{Na}^+$ | $y = 1.7275x + 185.79$ | 0.9956 | 1.7275 | 0.288                    |
| $\text{K}^+$  | $y = 2.777x - 93.042$  | 0.9949 | 2.777  | 0.463                    |
| $\text{Rb}^+$ | $y = 2.8637x + 83.015$ | 0.9988 | 2.8637 | 0.477                    |
| $\text{Cs}^+$ | $y = 3.307x + 134.54$  | 0.9959 | 3.307  | 0.551                    |

molecules in the model system is much larger than the number of alkali metal ions, and there is little difference with the number of water molecules formed by alkali metal ions.

As can be seen from Table 2, the linear coefficient  $R^2$  of  $MSD-t$  curve of  $\text{Li}^+$  is 0.9772, and  $R^2$  of the other four  $M^+$  are all greater than 0.99. It shows that the linear diffusion of  $\text{Li}^+$  is weaker than that of the other four alkali metal ions. The order of diffusion coefficients of the five  $M^+$  is  $\text{Cs}^+ > \text{Rb}^+ > \text{K}^+ > \text{Li}^+ > \text{Na}^+$ , indicating that except for  $\text{Li}^+$ , the larger the atomic radius, the stronger the diffusion of  $M^+$  during adsorption with GO/G composite. It is worth noting that the diffusion coefficient of  $\text{Li}^+$  is between  $\text{K}^+$  and  $\text{Na}^+$ , because the alkali metal ions combine with water molecules to form charged particles in an electrolyte solution. Due to the small radius of  $\text{Na}^+$ , the charge density is high and it can absorb more water molecules, resulting in the maximum radius of hydration ion. However, the  $\text{K}^+$  radius is large and the charge density is low, so the adsorption of water molecules is less than that of  $\text{Na}^+$ , so the hydration ion radius is smallest,  $\text{Li}^+$  is between them, that is,  $\text{Li}^+$  is abnormal in aqueous solution [32].

### 3.4. Radial distribution function

Radial distribution function (RDF) usually refers to the probability of the distribution of other particles in space given the coordinates of one particle. So the radial distribution function can be used not only to study the order of matter, but also to describe the correlation of electrons. For better understanding the interaction essence between atoms or molecules or between atoms and molecules in the model system, the bonding situation was analyzed by calculating the RDF [33]. Based on the possible interactions in the system, we calculated the RDFs between  $M^+$ -GO and between  $M^+$ -O(GO), respectively, as shown in Fig. 6.  $M^+$  and GO denote all the alkali metal ions and GO sheet in the model, respectively; O(GO) represents O atoms of the GO sheet, respectively.

As can be seen from Fig. 6a, RDFs between  $M^+$ -GO of five different  $M^+$  have roughly similar trends. At about 2.5 Å, except for  $\text{Li}^+$ , the RDFs between the other four  $M^+$  and GO show sharp peaks, while  $\text{Li}^+$  does not show any peaks before 3.5 Å. This indicates that in the short area, other

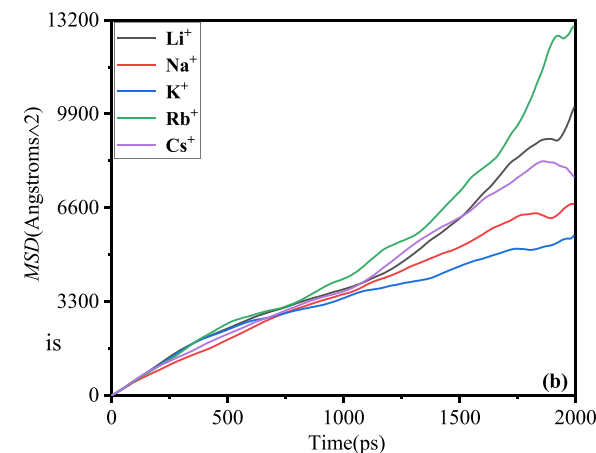


**Fig. 5.** MSD-t curves of  $M^+$ (a) and water (b) in the different  $M^+ - \text{GO}/\text{G}$  model systems.

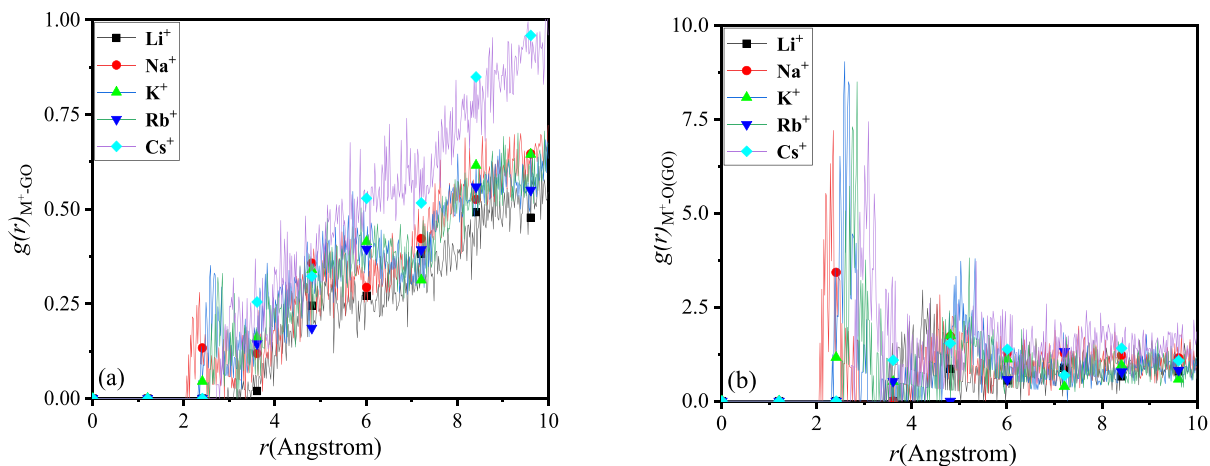


Fig. 6. RDF curves of between  $M^+$ -GO(a) and between  $M^+$ -O(GO)(b).

four  $M^+$  are prone to bond with GO, while  $\text{Li}^+$  is difficult to bond with GO. At about 6 Å, RDFs between  $M^+$ -GO of five different  $M^+$  show a significantly larger peak than that at 2.5 Å, and  $\text{Li}^+$  also shows a strong peak, indicating that the non-bonding interaction between  $M^+$ -GO in the model system is easy to form in the remote area. Moreover, the non-bonding is significantly larger than the bonding, indicating that the formation of the system in which  $M^+$  interact with GO is mainly provided by the non-bonding. The non-bonding interaction between  $\text{Cs}^+$  and GO is obviously larger, because the radius of  $\text{Cs}^+$  is obviously larger than that of the other four  $M^+$  with the increase of the radius of elements of the same race, and the charge density is the lowest, so the number of water molecules absorbed is also significantly smaller, that is, the radius of  $\text{Cs}^+$  hydration ion is the smallest. As a result,  $\text{Cs}^+$  is more likely to have non-bonding interaction with GO in the remote area. This is consistent with the variation trend of the diffusivity of alkali metal ions in solution in Section 3.3.

Fig. 6b showed the interaction of oxygen atoms of GO with  $M^+$ . It could be clearly seen from the image that  $\text{Na}^+$  first appeared an obvious

peak at 2.3 Å, followed by  $\text{K}^+$ ,  $\text{Rb}^+$  and  $\text{Cs}^+$  ions with strong peaks between 2.5 Å and 3.0 Å, while  $\text{Li}^+$  had the first obvious peak at 3.5 Å. It showed that different  $M^+$  bond with O atoms of GO in the short area, and its strength order is consistent with that of between  $M^+$ -GO. Because  $M^+$  is positively charged while O in GO is negatively charged. Fig. 7 displayed that the distance between  $\text{Rb}^+$  and the O atom of GO is significantly smaller than the distance between  $\text{Rb}^+$  and the GO sheet. As a result, they tend to form bonds due to electrostatic attraction in the near action region. It could also be seen from Fig. 7 that rubidium ions do not directly contact GO/G, but are surrounded by water molecules to form hydrated ions that indirectly interact with GO/G. Other alkali metal ions and rubidium ions interact similarly with GO. This indicates that the nature of adsorption of alkali metal ions on GO/G surface is a process of interaction between alkali metal hydration ions and GO/G surface. In the range of 3.5–10.0 Å, when the distance is about 5.0 Å, the second peak appears in all the  $M^+$  systems, however, it is much smaller than the first peak. This indicates that in the remote action region, the non-bonding interaction is much weaker than the bonding interaction,

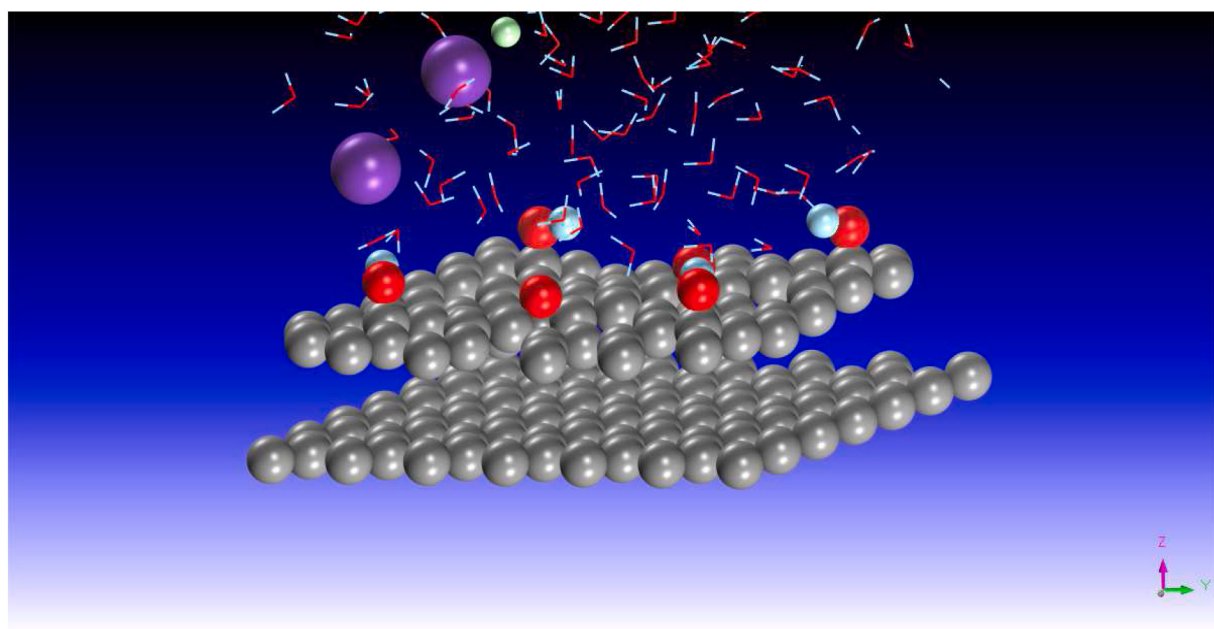


Fig. 7. The distribution of  $\text{Rb}^+$ ,  $\text{Cl}^-$  and  $\text{H}_2\text{O}$  molecules on the GO/G composite after molecular dynamics simulation of 2000 ps. The distance between  $\text{Rb}^+$  and O atom of GO is the shortest. Purple spheres denote  $\text{Rb}$  ions, cyan spheres denote  $\text{Cl}$  ions, line-type structures denote  $\text{H}_2\text{O}$  molecules, CPK models represents GO/G. (For interpretation of the references to colour in this figure legend, the reader is referred to the Web version of this article.)

which is due to the adsorption of  $M^+$  with  $H_2O$  molecules and the increase of the distance between  $M^+$  and O atoms of GO, and this electrostatic adsorption becomes very weak. The formation of the system in which alkali metal ions interact with O atoms of GO is mainly provided by bonding interaction.

#### 4. Conclusions

The interaction between different alkali metal ions and the GO/G composite electrode could be studied by MD simulation. The results showed that the adsorption process between  $M^+$  and the GO/G complex surface is mutual attraction. The GO/G complex structure has a greater adsorption activity for  $M^+$  with a larger radius. The larger the hydration ion radius of  $M^+$ , the stronger the diffusion of  $M^+$  during adsorption with GO/G. The non-bonding between  $M^+$  and GO was stronger than the bonding, and the bonding between  $M^+$  and the O atoms of GO was stronger than the non-bonding. The formation of the former interaction system is mainly provided by non-bonding interaction, while the latter is mainly provided by bonding interaction.

#### Declaration of competing interest

The authors declare that they have no known competing financial interests or personal relationships that could have appeared to influence the work reported in this paper.

#### Acknowledgments

We would like to acknowledge financial support from University-Industry Cooperation Research Project in Jiangsu (No. YG2020051405) and 2021 College Students Innovation Training Program Project of Yancheng Institute of Technology (School-enterprise Cooperation Projects, No. 100).

#### References

- [1] Z. Zheng, J. Yang, J. Guo, R. Shi, Preparation of graphene and its adsorption to Cr (VI), *Chin. J. Process Eng.* 17 (5) (2017) 1085–1090.
- [2] A. Feng, Y. Yu, L. Mi, Y. Yu, L. Song, Comparative study on electrosorptive behavior of  $NH_4HF_2$ -etched  $Ti_3C_2$  and HF-etched  $Ti_3C_2$  for capacitive deionization, *Ionics* 25 (2) (2019) 727–735.
- [3] W. Xing, J. Liang, W. Tang, G. Zeng, X. Wang, X. Li, L. Jiang, Y. Luo, X. Li, N. Tang, M. Huang, Perchlorate removal from brackish water by capacitive deionization: experimental and theoretical investigations, *Chem. Eng. J.* 361 (2019) 209–218.
- [4] J. Huang, D. Ding, Y. Li, Zhang H, H. Liu, Hu Y, X. Ye, Z. Wu, Preparation of pine needle based carbon electrode and its electrosorption of alkali/alkaline earth metal Ions , *Mater. For. Rep.* 34 (6) (2020) 12015–12019.
- [5] Q. Zhou, Y. Wang, J. Xiao, H. Fan, Fabrication and characterisation of magnetic graphene oxide incorporated  $Fe_3O_4$ @polyaniline for the removal of bisphenol A, t-octyl-phenol, and  $\alpha$ -naphthol from water, *Sci. Rep.* 7 (2017) 11316.
- [6] H. Tang, Y. Zhao, S.J. Shan, X.N. Yang, D.M. Liu, F.Y. Cui, B.S. Xing, Theoretical insight into the adsorption of aromatic compounds on graphene oxide, *Environ. Sci. Nano* 5 (10) (2018) 2357–2367.
- [7] C. Zhao, J. Jin, Y. Huo, L. Sun, Y. Ai, Adsorption of phenolic organic pollutants on graphene oxide: molecular dynamics study, *J. Inorg. Mater.* 35 (3) (2020) 277–283.
- [8] H. Liu, D. Ding, Z. Qian, Y. Hu, X. Ye, Z. Wu, Adsorption of alkali metal ions by biomass carbon aerogel-graphene oxide composite electrode, *Technol. Water Treat.* 46 (10) (2020) 21–24.
- [9] C. Zhao, H. Shan, S. Peng, C. Zeng, Adsorption of Cr(VI) in water by iron loaded graphene oxide chitosan, *Technol. Water Treat.* 3 (2) (2021) 45–51.
- [10] Y. Ou, B. Yuan, W. Li, Preparation of graphene oxide modified starch and its adsorption performance of  $Cu^{2+}$  and  $Pb^{2+}$ , *Environ. Pollut. Control.* 40 (12) (2018) 1412–1417.
- [11] B. Akgöz, O. Civalek, Thermo-mechanical buckling behavior of functionally graded microbeams embedded in elastic medium, *Int. J. Eng. Sci.* 85 (2014) 90–104.
- [12] B. Akgöz, O. Civalek, A size-dependent shear deformation beam model based on the strain gradient elasticity theory, *Int. J. Eng. Sci.* 70 (2013) 1–14.
- [13] L. Liu, J. Liu, J. Pei, Towards a better understanding of adsorption of indoor air pollutants in porous media—from mechanistic model to molecular simulation, *Build. Simulat.* 11 (2018) 997–1010.
- [14] Z. Taheri, A.N. Pour, Studying of the adsorption and diffusion behaviors of methane on graphene oxide by molecular dynamics simulation, *J. Mol. Model.* 27 (2) (2021) 59.
- [15] Q.B. Li, Y.T. Xiao, X.Y. Shi, S.F. Song, Rapid evaporation of water on graphene/graphene-oxide: a molecular dynamics study, *Nanomaterials* 7 (9) (2017) 265.
- [16] M.S. Izadkhah, H. Erfan-Niya, S.Z. Heris, Influence of graphene oxide nanosheets on the stability and thermal conductivity of nanofluids Insights from molecular dynamics simulations, *J. Therm. Anal. Calorim.* 135 (1) (2019) 581–595.
- [17] Y. Yang, D. Zhong, Y.L. Liu, D.H. Meng, L.N. Wang, N. Wei, G.H. Ren, R.X. Yan, Y. Kang, Thermal transport in graphene oxide films: theoretical analysis and molecular dynamics simulation, *Nanomaterials* 10 (2) (2020) 285.
- [18] Y. Yang, J. Cao, N. Wei, D.H. Meng, L.N. Wang, G.H. Ren, R.X. Yan, N. Zhang, Thermal conductivity of defective graphene oxide: a molecular dynamic study, *Molecules* 24 (6) (2019) 1103.
- [19] P. Wang, G. Qiao, Y.P. Guo, Y. Zhang, D.S. Hou, Z.Q. Jin, J.R. Zhang, M.H. Wang, X.X. Hu, Molecular dynamics simulation of the interfacial bonding properties between graphene oxide and calcium silicate hydrate, *Construct. Build. Mater.* 260 (2020) 119927.
- [20] B. Zheng, Y.M. Tian, S.C. Jia, X. Zhao, H. Li, Molecular dynamics study on applying layered graphene oxide membranes for separating cadmium ions from water, *J. Membr. Sci.* 603 (2020) 117996.
- [21] H. Sun, COMPASS: an ab initio force-field optimized for condensed-phase applications overview with details on alkane and benzene compounds, *J. Phys. Chem. B* 102 (38) (1998) 7338–7364.
- [22] S.W. Bunte, H. Sun, Molecular modeling of energetic materials: the parameterization and validation of nitrate esters in the COMPASS force field, *J. Phys. Chem. B* 104 (11) (2000) 2477–2489.
- [23] J. Zeng, H. Chen, C. Zhou, H. Liu, S. Chen, Molecular dynamics study at  $N_2/H_2O$ -rGO interfaces for nitrogen reduction reaction, *J. Mol. Graph. Model.* 104 (2021) 107840.
- [24] J. Liu, P. Li, H. Xiao, Y. Zhang, X. Shi, X. Lü, X. Chen, Understanding flocculation mechanism of graphene oxide for organic dyes from water: experimental and molecular dynamics simulation, *AIP Adv.* 5 (11) (2015) 117151.
- [25] Y. Sun, L. Chen, L. Cui, Y. Zhang, X. Du, Molecular dynamics simulation of the effect of oxygen-containing functional groups on the thermal conductivity of reduced graphene oxide, *Comput. Mater. Sci.* 148 (2018) 176–183.
- [26] A. Nicolai, P. Zhu, B.G. Sumpter, V. Meunier, Molecular dynamics simulations of graphene oxide frameworks, *J. Chem. Theor. Comput.* 9 (2013) 4890.
- [27] J. Zeng, Y. Zhang, R. Sun, S. Chen, Electroreduction property and MD simulation of nitrobenzene in ionic liquid [BMim][Tf<sub>2</sub>N]/[BMim][BF<sub>4</sub>], *electrochim. Acta* 134 (2014) 193–200.
- [28] H.J. Berendsen, J. Postma, W.F. van Gunsteren, A. DiNola, J. Haak, Molecular dynamics with coupling to an external bath, *J. Chem. Phys.* 81 (8) (1984) 3684–3690.
- [29] J. Zeng, J.Y. Zhang, X.D. Gong, Molecular dynamics simulation of interaction between benzotriazoles and cuprous oxide crystal, *Comput. Theor. Chem.* 963 (1) (2011) 110–114.
- [30] T. Chakraborty, A. Hens, S. Kulashrestha, N.C. Murmu, P. Banerjee, Calculation of diffusion coefficient of long chain molecules using molecular dynamics, *Physica E* 69 (2015) 371–377.
- [31] G.B.A. Chen, Z.W. Liu, Effect of modification on the fluid diffusion coefficient in silica nanochannels, *Molecules* 26 (13) (2021) 4030.
- [32] S. Gao, S. Chen, G. Xie, Periodic Table of the Elements, fourth ed., Science Press, 2016.
- [33] J. Zeng, L. Chen, Y. Xu, S. Chen, Diffusion mechanism of nitrobenzene in hydrophilic, hydrophobic, and their composite ionic liquids, *Prot. Met. Phys. Chem.* +. 56 (5) (2020) 886–896.